AD-A160 143 LASER PHYSICS AND LASER TECHNIQUES(U) STANFORD UNIV CA 1/1
EDWARD L GINZTON LAB OF PHYSICS A E SIEGMAN ET AL.
14 MAY 85 AFOSR-TR-85-0882 F49620-84-C-0041
UNCLASSIFIED F/G 20/12 NL

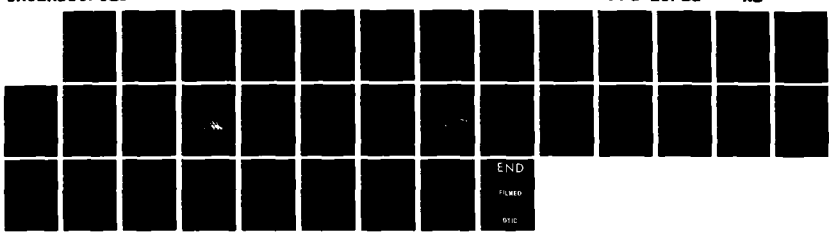

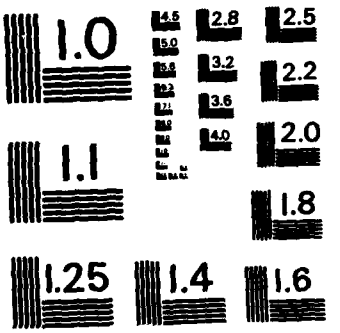

MICROCOPY RESOLUTION TEST CHART
NATIONAL BUREAU OF STANDARDS - 1963 - A

UNCLASSIFIED

SECURITY CLASSIFICATION OF THIS PAGE

AD-A160143

REPORT DOCUMENTATION PAGE

1a. REPORT SECURITY CLASSIFICATION: Unclassified	1b. RESTRICTIVE MARKINGS
2a. SECURITY CLASSIFICATION AUTHORITY	3. DISTRIBUTION/AVAILABILITY OF REPORT: Unlimited Approved for public release; distribution unlimited.
2b. DECLASSIFICATION/DOWNGRADING SCHEDULE	
4. PERFORMING ORGANIZATION REPORT NUMBER(S)	5. MONITORING ORGANIZATION REPORT NUMBER(S): AFOSR-TR- 85-0882
6a. NAME OF PERFORMING ORGANIZATION: Stanford University; 6b. OFFICE SYMBOL (If applicable)	7a. NAME OF MONITORING ORGANIZATION: Air Force Office of Scientific Research
6c. ADDRESS (City, State and ZIP Code): Edward L. Ginzton Laboratory, Stanford, California 94305	7b. ADDRESS (City, State and ZIP Code): Directorate of Physical and Geophysical Sciences, Bolling AFB, DC 20332
8a. NAME OF FUNDING/SPONSORING ORGANIZATION: AFOSR; 8b. OFFICE SYMBOL (If applicable): NP	9. PROCUREMENT INSTRUMENT IDENTIFICATION NUMBER: Contract F49620-84-C-0041
8c. ADDRESS (City, State and ZIP Code): Bolling AFB, DC 20332	10. SOURCE OF FUNDING NOS.

PROGRAM ELEMENT NO.	PROJECT NO.	TASK NO.	WORK UNIT NO.
61102F	2301	A1	

11. TITLE (Include Security Classification): Laser Physics and Laser Techniques (unclassified)

12. PERSONAL AUTHOR(S): SIEGMAN, Anthony E., Trebino, R., Fouquet, J.E., P.M. Fauchet

13a. TYPE OF REPORT	13b. TIME COVERED	14. DATE OF REPORT (Yr., Mo., Day)	15. PAGE COUNT
Int. Scientific Reprt.	FROM 84/3/1 TO 85/2/28	1985 May 14	33

16. SUPPLEMENTARY NOTATION

17 COSATI CODES		
FIELD	GROUP	SUB. GR.

18. SUBJECT TERMS (Continue on reverse if necessary and identify by block number)
Lasers; Polarization Spectroscopy; Femtosecond spectroscopy; Optical Homodyne Detection; Thermal gratings; Laser-Solid Interactions /over...

19. ABSTRACT (Continue on reverse if necessary and identify by block number)

A basic research program on optical physics and techniques proceeded very well. Research involving femtosecond-process measurement in the frequency domain, laser surface transformations and damage mechanisms, the study of specific quantum-well structures, and the development of optical beam expanders ~~all~~ resulted in significant achievements during the ~~past year~~. In particular, attempts to suppress troublesome thermal-grating effects in frequency-domain measurements of femtosecond processes produced two entirely different--and successful--techniques, each of which yields other advantages as well. Our studies of laser-solid interactions have led to a better understanding of transient electronic processes in very dense and hot electron-hole plasmas in semiconductors and of the formation of single-laser-beam-induced spontaneous surface ripples on a multitude of solid materials. ~~In~~ our time-resolved studies of GaAs/$Al_xGa_{1-x}As$ quantum well structures, we successfully measured the photoluminescence decay times of carriers in structures grown by both molecular beam epitaxy and metalorganic chemical vapor deposition. Much

20. DISTRIBUTION/AVAILABILITY OF ABSTRACT	21. ABSTRACT SECURITY CLASSIFICATION
UNCLASSIFIED/UNLIMITED ☒ SAME AS RPT ☐ OTIC USERS ☐	Unclassified

22a. NAME OF RESPONSIBLE INDIVIDUAL	22b. TELEPHONE NUMBER (Include Area Code)	22c. OFFICE SYMBOL
Dr. Schlossberg	(202) 767-4960	NP

DD FORM 1473, 83 APR EDITION OF 1 JAN 73 IS OBSOLETE.

Unclassified

SECURITY CLASSIFICATION OF THIS PAGE

18. Continued

Quantum well
Multiple quantum well
Excitons
Time-resolved photoluminescence
Photoluminescence
GaAs
Single photon counting
Prism beam expanders

19. Abstract (contd.)

was learned about the nature of nonradiative recombination dynamics in these structures. Results consistently indicated that the fundamental radiative recombination coefficient, B, in quantum wells is quite small ~~(on the order of a few times 10^{11})~~. ~~Finally, we developed~~ optimal designs for achromatic prism beam expanders, based on a remarkably simple and elegant theoretical analysis of what appears at first to be a complex and unwieldy problem amenable to numerical techniques only.

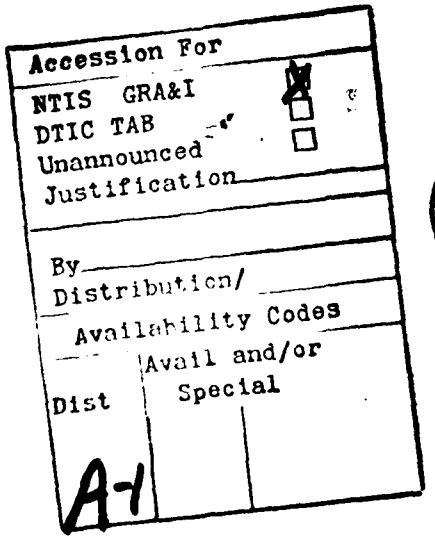

TABLE OF CONTENTS

Chief, Te... ...ion

I. INTRODUCTION

This is the Interim Scientific Report on AFOSR Contract F49620-84-C-0041 for the period 1 March 1984 through 28 February 1985. This report summarizes research, journal publications, and conference presentations relating to tunable-laser-induced-grating spectroscopy, laser-induced surface transformations and spontaneous "ripples," time-resolved studies of quantum-well structures, and achromatic prism beam expanders. A complete list of AFOSR-sponsored publications and conference presentations is attached.

II. REVIEW OF ACCOMPLISHMENTS

A. Tunable-Laser-Induced-Grating Spectroscopy

Probably the longest-running and most novel research effort under this contract has been tunable-laser-induced-grating spectroscopy, or, equivalently, variable-frequency four-wave-mixing, a technique that allows measurements of femtosecond events without the need for femtosecond pulses—in fact, the technique yields its best results in this regime—using nanosecond or longer pulses. In the past, we have made accurate measurements on optical-Kerr liquids and triphenyl methane dyes in aqueous solution. But, while these results have been both exciting and encouraging, a problem has plagued the technique, limiting its use to transparent materials and absorbing materials in high-thermal-conductivity solvents or host materials: this problem is the phenomenon of the simultaneous formation of the desired material grating and an undesired *thermal grating*, the latter of which usually obscures the desired ultrafast information. Researchers have developed various techniques to suppress the thermal-grating effects (for example, using very dilute solutions), but these methods have had little sound theoretical basis and even less success.

1. Suppression of thermal gratings by optical homodyne detection using partially coherent light

A frequency-domain technique that is particularly popular is the polarization-spectroscopy method demonstrated by Song *et. al.*[1] This method is easy to align, is nearly background-free, and yields theoretically the relaxation time(s) of the probed transition, including the dephasing time. Its main drawback, like that of all other frequency-domain geometries, however, has been the presence of the above-mentioned thermal gratings.

Suppression of the thermal-grating signal cannot be achieved by the manipulation of experimental parameters, since both population and thermal-grating signals have nearly identical theoretical dependences on concentration, sample interaction length, experimental wavelengths, and laser intensities. The coherence properties of the excitation lasers do, however, appear differently in theoretical expressions. If the excitation laser fields are written as $\mathcal{E}_i(t) = \mathrm{Re}\, E_i(t) \exp(i\omega_i t)$, then the population signal field in the polarization-spectroscopy arrangement will be

$$k_{pop}(t) \propto \chi^{(3)}_{pop} [E_1(t) E_2^*(t)] E_2(t) = \chi^{(3)}_{pop} |E_2(t)|^2 E_1(t)\,, \tag{1}$$

where the bracketed quantity is a population grating strength and the material response, τ is assumed nearly instantaneous, i.e., much less than the radiation coherence time, τ_c, and pulse length, τ_p. The thermal grating exhibits a much longer relaxtion time, τ_{th}, which is generally much longer than the pulse length. Thus, the thermal-grating signal field will be

$$E_{th}(t) \propto \chi^{(3)}_{th}\left[\frac{1}{\tau_p}\int_{-\infty}^{t} E_1(t')E_2^*(t'))\,dt'\right]E_2(t). \tag{2}$$

In the coherent limit (E_i independent of time), the bracketed grating factors in Eqs. (1) and (2) are identical, with each signal field proportional to $|E_2|^2E_1$. The use of only partially coherent light, on the other hand, allows some cancellation and phase randomization to occur in the integral of Eq. (2), reducing the thermal-grating strength but not the population effect.

We showed that additional suppression can be achieved by employing the optical heterodyne method. Optical homodyning[2] involves the presence of a local-oscillator field [here, a piece of $E_1(t)$] and the observation of cross terms between this field and the signal field(s) rather than the observation of signal intensities (which are now negligible in comparison). Homodyne detection, by singling out only those signal fields in phase with it, will preferentially extract the population signal field because it also has its phase given by $E_1(t)$. When the excitation radiation is only partially coherent, this will still be the case, but the local-oscillator field will be only partially coherent with the thermal-grating signal field, and suppression of this effect occurs. If the ratio of population to thermal-grating intensities is r without optical homodyning, we show that homodyning with partially coherent light yields an improvement in this value by a factor of $(2\tau_p/r\tau_c)^{1/2}$, which can be quite large, especially when the radiation coherence time, τ_c, is small, i.e., the radiation is minimally coherent. In addition, the most improvement occurs when r is small—when it is most needed. Finally, optical homodyning can be combined with other methods of thermal-grating suppression,[3] while retaining the inherent advantages of optical homodyning [2] (improved signal-to-noise ratio and the individual measurements of the real and imaginary parts of the susceptibility).

We have applied these techniques to the measurement of population relaxation effects of organic dyes in solution: azulene and various triphenylmethane dyes dissolved in chloroform and hexane. In previous experiments on these materials, thermal gratings have dominated, preventing the extraction of relaxation time scales. Our experi-

ments, reported at the 13th International Quantum Electronics Conference at Anaheim, California, confirmed the significant reduction in the thermal-grating contribution to the observed signal by as much as a factor of 100. With such reductions in thermal-grating strengths, we were able to measure the excited-state subpicoscond lifetimes of such molecules as malachite green, crystal violet, and ethyl violet in the formerly unusable solvents such as ethanol, methanol, and chloroform.[4]

2. Suppression of thermal gratings using orthogonally polarized excitation beams

An even better method for the suppression of thermal gratings exists; it involves the use of orthogonally polarized excitation beams. While not as intuitive as the formation of gratings with beams of the same polarization, the interface of beams or orthogonally polarized light produce *orientational* gratings, which exhibit similar diffraction efficiencies for gratings of vector quantities. Excited states, whose dipole nature represents a vector quantity, form such orientational gratings. Thermal gratings, on the other hand, are gratings of a scalar quantity, the temperature, which exhibits a uniform spatial distribution when orthogonally polarized excitation beams interfere, and, as a result, significant suppression of this thermal effect occurs. This technique has been employed in time-domain work, where thermal gratings have not been such a dramatic problem; we recognized the increased importance of this method for frequency-domain work.

We reported at *LASERS* '84 in San Francisco, California on our orthogonal-polarization experiments, which demonstrated thermal-grating suppression quite dramatically in all cases. Solvents such as methanol, ethanol, and chloroform, which had always shown thermal components that completely obscured the desired population components, revealed excited-state gratings with very little or no thermal component at all (See Figs. 1 and 2). These experiments allowed high-signal-to-noise excited-state-decay measurement in the femtosecond regime, where such dynamics had been unobservable previously. In addition, we were able to curve-fit the resulting data to complex sum-of-exponentials decays but not single-exponential decays, indicating rather complex molecular dynamics in all cases.

These experiments represent a breakthrough in femtosecond technology. With the frequency-domain technique, we can now obtain temporal resolution on the order of 1 fsec, using reliable Q-switched-laser technology, without troublesome experimental artifacts.

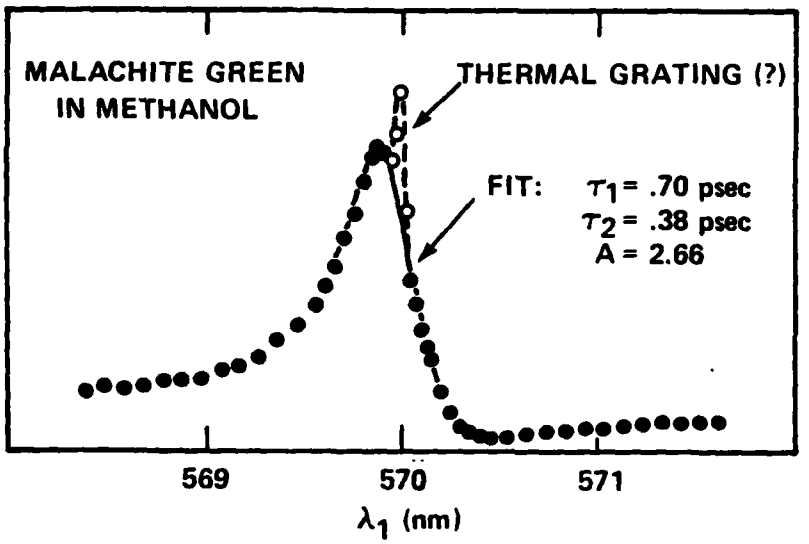

FIGURE 1

Tunable-laser-induced-grating study on malachite green in methanol using orthogonal excitation polarizatrions. Data have been fit to a decay law of the form: $h(t) = A\exp(-t/\tau_1) + (1-A)\exp(-t/\tau_2)$.

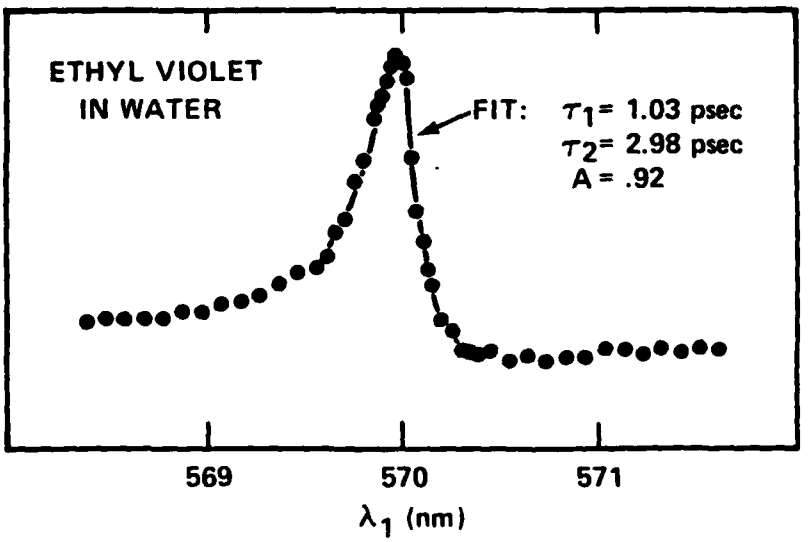

FIGURE 2

Tunable-laser-induced grating study on ethyl violet in water using orthogonal excitation polarizations. Data have been fit to a decay law of the form: $h(t) = A\exp(-t/\tau_1) + (1-A)\exp(-t/\tau_2)$.

B. Laser-Solid Interactions

This effort, which was started in 1981, was continued last year by Philippe Fauchet who was the IBM Post-doctoral Fellow at the Ginzton Laboratory, and by Dan Dale, an undergraduate physics major working on his senior thesis.

The first major focus of this research effort was to better understand the transient electronic processes that take place when very dense ($\gtrsim 10^{20}$ cm^{-3}) and very hot ($\gtrsim 200°$ K) electron-hole plasmas are produced in semiconductors. Two and a half years ago, we introduced a novel technique to study these processes in detail. Our two-color excitation (TCE) technique proved to be very sensitive to electronic temperature, carrier density and free-carrier absorption in ion-implanted silicon. Starting in 1984, we have extended such measurements to intrinsic silicon and ion-implanted gallium arsenide, two materials for which accurate measurements had proved in the past to be more difficult to obtain. We also refined our theoretical modeling in all materials. The details of our recent experimental and theoretical findings have been presented at the Topical Meeting on Ultrafast Phenomena (Monterey, June 1984), and at the 17th International Conference on the Physics *of* Semiconductors (San Francisco, August 1984). The results and modeling for intrinsic silicon are also presented in the B.S. thesis of Dan Dale (June 1984). Among the interesting results, we found that the presence of a dense and hot plasma opened new absorption channels between the densely populated lower lying conduction band and higher lying conduction bands. Also, the importance of carrier diffusion was much larger in intrinsic materials than in disordered materials, with a characteristic time of ≈ 100 psec. This study has clearly helped the thermal model of pulsed laser annealing. It also has given us access to quantities which had never been measured in a quantitative way in such highly excited materials.

The second major focus of this research effort was to understand and model the transformations induced on the surface of semiconductors by single or multiple high power laser pulses. Specifically, we continued our pioneering effort in the field of laser-induced ripples. The results of our recent experiments and calculations were presented at the International Quantum Electronics Conference (Anaheim, June 1984), and at the Annual Meeting of the Materials Research Society (Boston, November 1984). We have specially focussed our attention on the ripple structures that are not presently explained by any theory. Our careful characterization of their properties has led us to speculate on their origin. Due to the formidable mathematical difficulties in describing these highly nonlinear interactions

which couple dynamically to large material's modifications, we have not attempted to present a detailed theory that would complement our previously published model. The growth of these ripples under repetitive illumination, and the production of other damage morphologies by multiple subthreshold pulses, has also attracted some attention lately. We have summarized our results at the 16th Annual Symposium on Optical Materials for High Power Lasers (Boulder, October 1984).

This research program is now being discontinued at Stanford. Philippe Fauchet, who was responsible for this experimental and theoretical effort, accepted a faculty position in the EECS Department at Princeton University starting in September 1984 where some of these investigations will continue, using novel techniques. Dan Dale is now a graduate student in the Physics Department at the University of Illinois, Urbana, Champaign.

C. Recombination Dynamics in GaAs/$Al_xGa_{1-x}As$ Quantum Well Structures Grown by Molecular Beam Epitaxy and Metalorganic Chemical Vapor Deposition

1. Summary

During the last year significant progress has been made in the area of time-resolved photoluminescence of GaAs/$Al_xGa_{1-x}As$ quantum well structures. An experiment using time-resolved single photon counting detection was set up. Quantum well structures grown by molecular beam epitaxy (MBE) and metal-organic chemical vapor deposition (MOCVD) were studied over a wide range of excitation densities.

Room temperature dynamics in the MBE multiple quantum well sample were dominated by nonradiative recombination, but the results were quite significant because they showed that free carriers, not excitons, are responsible for radiative recombination at 300 K. Further investigation of the photon energy of the photoluminescence peak versus temperature also supported this conclusion. This information helped resolve a conflict which arose in the summer of 1984 over whether free carriers or excitons were responsible for radiative recombination at room temperature.

A similar structure grown by MOCVD showed very different dynamics. At room temperature, dynamics at low excitation were controlled by traps, but at high excitation levels the traps could be saturated, leading to high photoluminescence efficiency with surprisingly slow decays. An unusual increase in photoluminescence decay rate was observed, which may be related to the MOCVD growth process, since this was the *first* study to inves-

tigate time-resolved photoluminescence of MOCVD-grown multiple quantum well structures. This increase in decay rate can be explained by carriers falling out of trap states. A rate equation model incorporating these effects has been developed and preliminary results are in qualitative agreement with the experimental results.

It was not possible to directly measure the radiative recombination coefficient B, but results from samples grown by both methods indicate that B is surprisingly small for quantum wells.

2. Experiment

Figure 3 illustrates the apparatus used to perform these experiments. Optical pulses approximately 200ps wide separated by 12ns intervals were provided by an actively modelocked Krypton ion laser. The repetition rate of the excitation pulses was reduced by an acousto-optic switch (Bragg cell) as necessary to allow complete photoluminescence decay before reexcitation, and to accommodate the 1MHz limit of the detection electronics. The laser and Bragg cell were rented from the San Francisco Laser Center (funded at the time by NSF) since our group did not possess an adequate laser system for this purpose at the time this experiment was initiated. The excitation pulse was attenuated by variable amounts before hitting the sample. Photoluminescence from the sample was collected with an objective and passed through a transfer lens to modematch into a 1/4-m monochromator. The monochromator output was focused onto the photocathode of a Hamamatsu R636-P photomultiplier tube. The monochromator could be driven while passing the photomultiplier output through a slow amplifier to obtain time-integrated spectra.

For time-resolved single photon counting detection, the monochromator was set at a wavelength of interest, and the signal from a single photon in the photomultiplier tube was amplified with fast amplifiers and discriminated. A reference timing pulse was obtained from the Bragg cell drive and discriminated. These two discriminated timing pulses functioned as start and stop pulses for a time to pulse height convertor, which output a voltage pulse whose height corresponded to the time elapsed between the two timing pulses. Amplifiers, discriminators, the time to pulse height convertor and a NIM bin were borrowed from the Van de Graaff Accelerator group in the Stanford Physics Department. The voltage pulse from the time to pulse height convertor was delivered to a multichannel analyzer. Data from many single photons were collected to make histograms

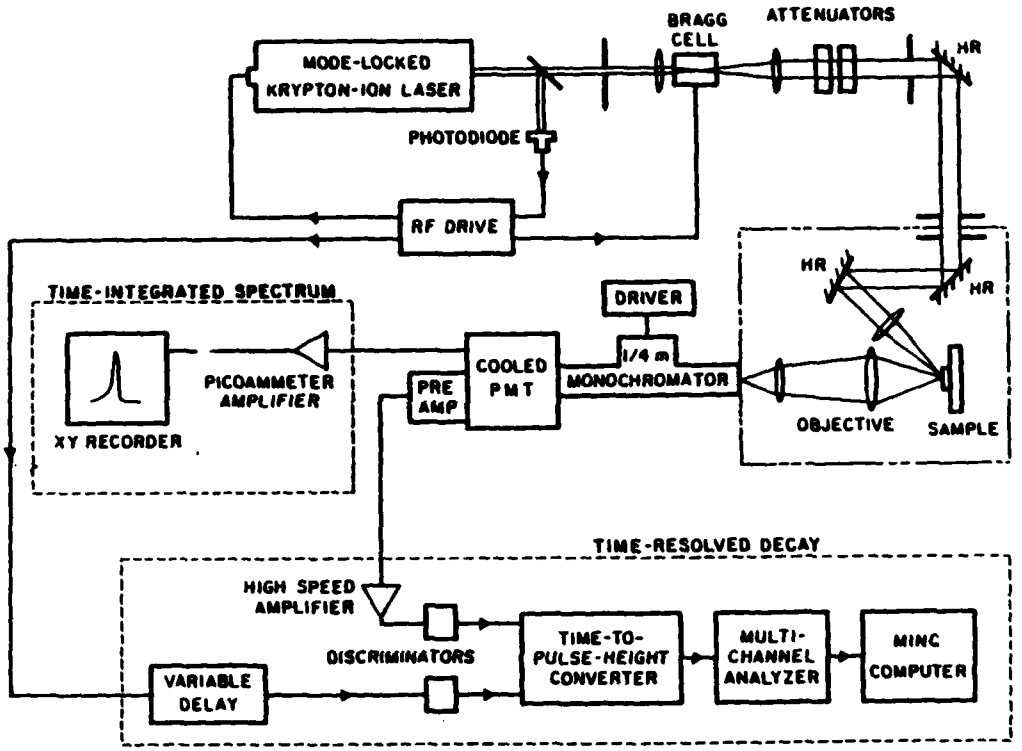

FIGURE 3

Repetition rate of pulses from a krypton-ion laser was reduced by a Bragg diffractor before exciting the sample. The photomultiplier signal was either discriminated to measure time-resolved photoluminescence decay or integrated to record the time-integrated spectrum.

representing the photoluminescence decay. The ability to count single photons makes this technique highly sensitive, and photoluminescence decay can be followed over many orders of magnitude. In addition, the use of fast amplification and discriminators gives this technique very good time resolution, down to an ultimate limit on the order of a few hundred picoseconds.

3. Molecular Beam Epitaxy Results

The MBE multiple quantum well sample was grown by A.C. Gossard at AT&T Bell Laboratories in Murray Hill, NJ. The active region consisted of 100 100Å GaAs wells between 200Å $Al_{.26}Ga_{.74}As$ barriers. Transparent minisuperlattice cladding regions were on either side. The active region was not intentionally doped. Pure GaAs grown in this system has a typical net carrier concentration less than 5×10^{15} cm^{-3}. Figure 4 illustrates the calculated energy levels for a quantum well with these parameters. In this figure the horizontal axis lies in the direction of growth of the layers.

The room temperature photoluminescence spectrum of this sample is shown in Fig. 5. Overall, the strength of this peak is quite weak. The steep low energy side is due to the quantum mechanical confinement in the growth direction. The gradual slope of the high energy side is due to the momentum of carriers in the infinite planes perpendicular to the direction of growth. The main peak is due to the $n = 1$ heavy hole transition, while the feature on the high energy side is due to the $n = 1$ light hole transition. At lower temperatures this feature becomes a separate peak, allowing measurement of the separation between the light and heavy hole peaks. This separation agrees well with the separation calculated using a program we have developed.

Time-resolved photoluminescence of the $n = 1$ heavy hole transition is shown in Fig. 6 for a number of different excitation densities. A decay time of approximately 1 ns is observed, and the decay time does not depend strongly on excitation density. Figure 7 illustrates time-integrated photoluminescence (area under the time-integrated spectrum) as a function of excitation density. The data fall on a line of slope two, indicating that time-integrated photoluminescence goes as the square of excitation density. These results can be explained by bimolecular (both electron and hole populations vary) free carrier radiative recombination in the limit where carrier population decay is dominated by nonradiative recombination. Neither monomolecular (only one kind of carrier population varies, while the other is fixed at a high level) recombination, nor simple free exciton (an exciton is

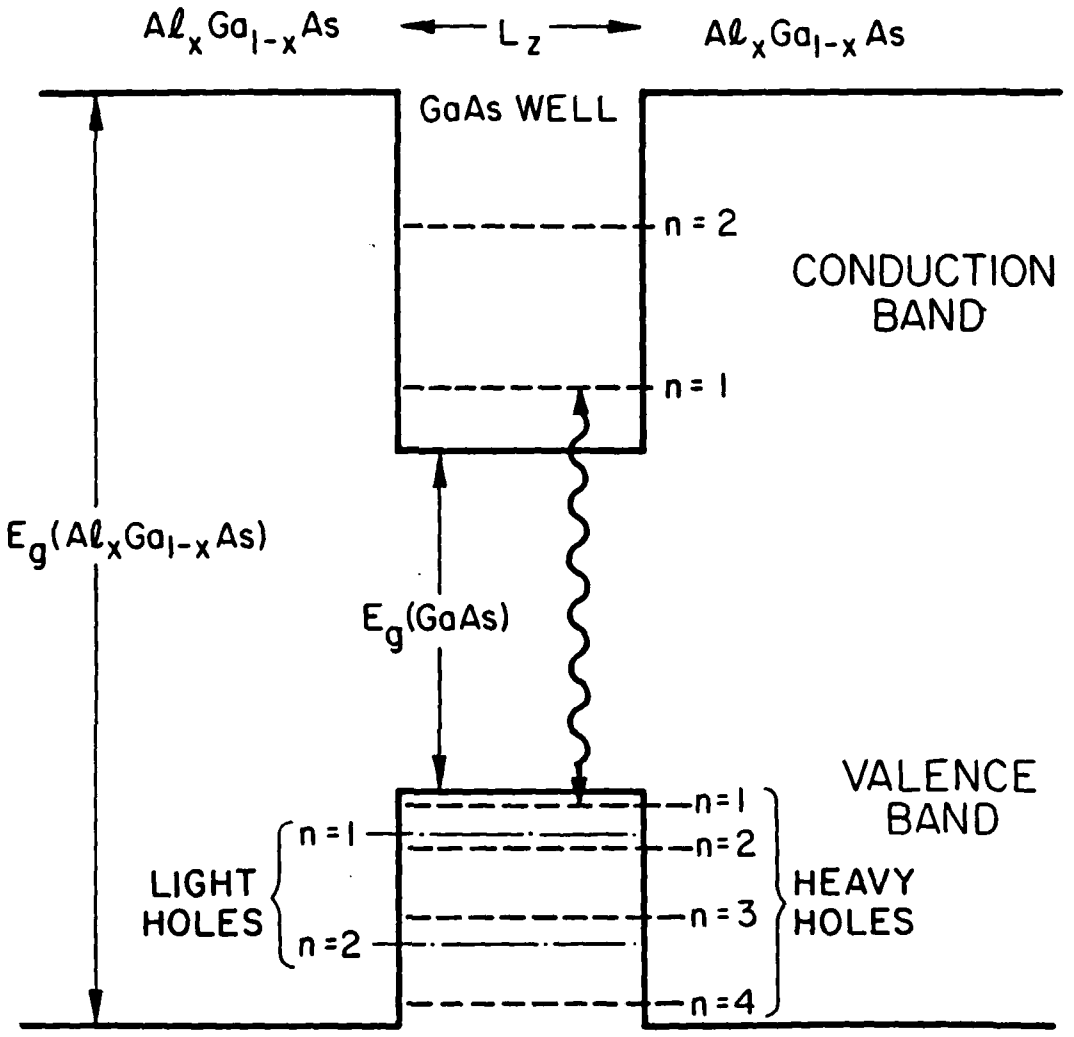

FIGURE 4

Energy levels in a 100Å wide GaAs well between $Al_{.25}Ga_{.75}As$ barriers grown for this work.

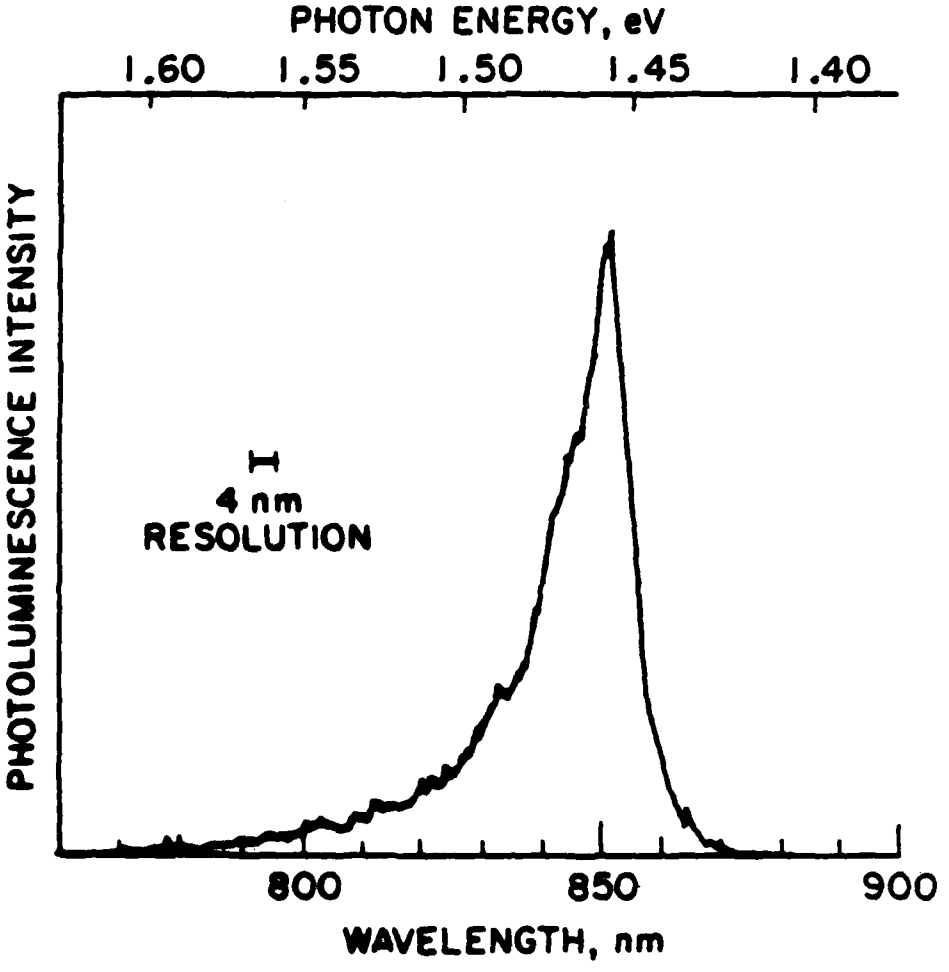

FIGURE 5

Time-integrated photoluminescence spectrum: excitation density is 17 $\mu J/cm^2$, resolution is 4 nm.

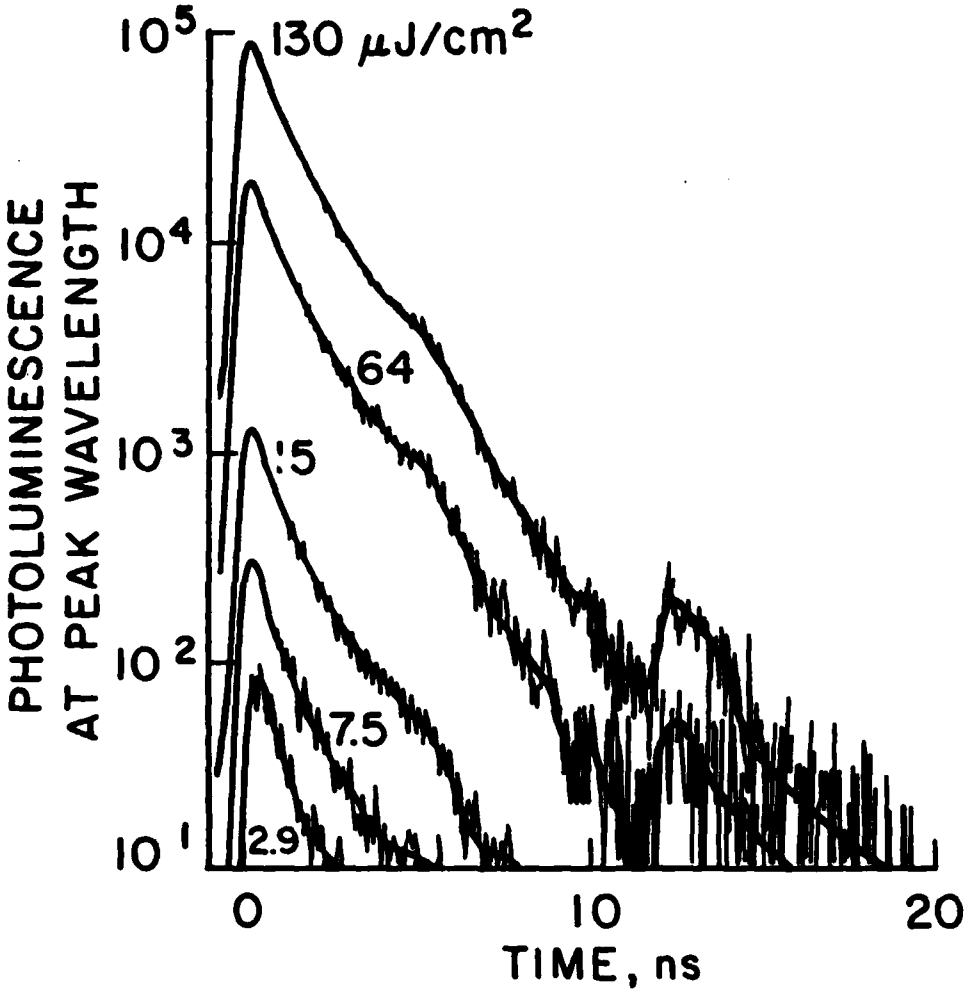

FIGURE 6

Time-resolved photoluminescence intensity (arbitrary units) at the peak wavelength exhibits a 1-ns exponential decay over nearly two orders of magnitude in excitation density. (The second peak and the hump which appears between one and two orders of magnitude down from the main peak are related to the impulse response structure).

a bound electron-hole pair) recombination can yield a slope of two for time-integrated photoluminescence as a function of excitation density. Thus these data indicate that room temperature radiative recombination in quantum wells is due to free carriers, not excitons. The fact that the slope remains two up to the highest excitation level indicates that the nonradiative mechanism has not yet been saturated. This information can be used to put an upper limit on the radiative recombination coefficient B of 5×10^{-10} cm^3/sec.

The conclusion of free carrier recombination is further supported by the data shown in Fig. 8, which illustrate the photon energy of the photoluminescence peak as a function of temperature. At low temperatures, recombination is generally accepted to be excitonic, so the data points (open circles) at low temperatures represent excitonic photoluminescence. The heavy line at low photon energies is the bandgap of GaAs as a function of temperature given by Casey and Panish.[5]. This curve is shifted to meet the data at low temperature, representing the increase in energy due to confinement in the quantum well minus the binding energy of the excitons. As the temperature increases, the data depart from this curve to an energy roughly 8 meV above the transposed curve. This shift is just the binding energy of the exciton in a quantum well of these parameters, so the excitons are ionizing at a temperature less than 50 K and recombination at room temperature is between free carriers. The work illustrated in Figs. 6–8 was significant in resolving a question which arose in the summer of 1984 over whether free carriers or excitons are responsible for room temperature radiative recombination.[6]

4. Metalorganic Chemical Vapor Deposition Results

The MOCVD samples were grown by R.D. Burnham at the Xerox Palo Alto Research Center. The multiple quantum well sample described here had nominally the same well and barrier dimensions as the MBE sample described above, but the barrier composition was slightly different, $Al_{.24}Ga_{.76}As$ and only 40 periods were grown. $Al_{.5}Ga_{.5}As$ material was grown on either side of the active region and functioned as a transparent cladding. A Polaron profile taken at Xerox measured a background carrier concentration in the active region of 2×10^{16} cm^{-3} n-type, which may be an underestimate. The room temperature time-integrated photoluminescence spectrum is quite similar in shape to the MBE spectrum, but the $n = 1$ light hole transition cannot be resolved and another feature is present at high photon energy which cannot be described by any of the transitions predicted by the simple square well model.

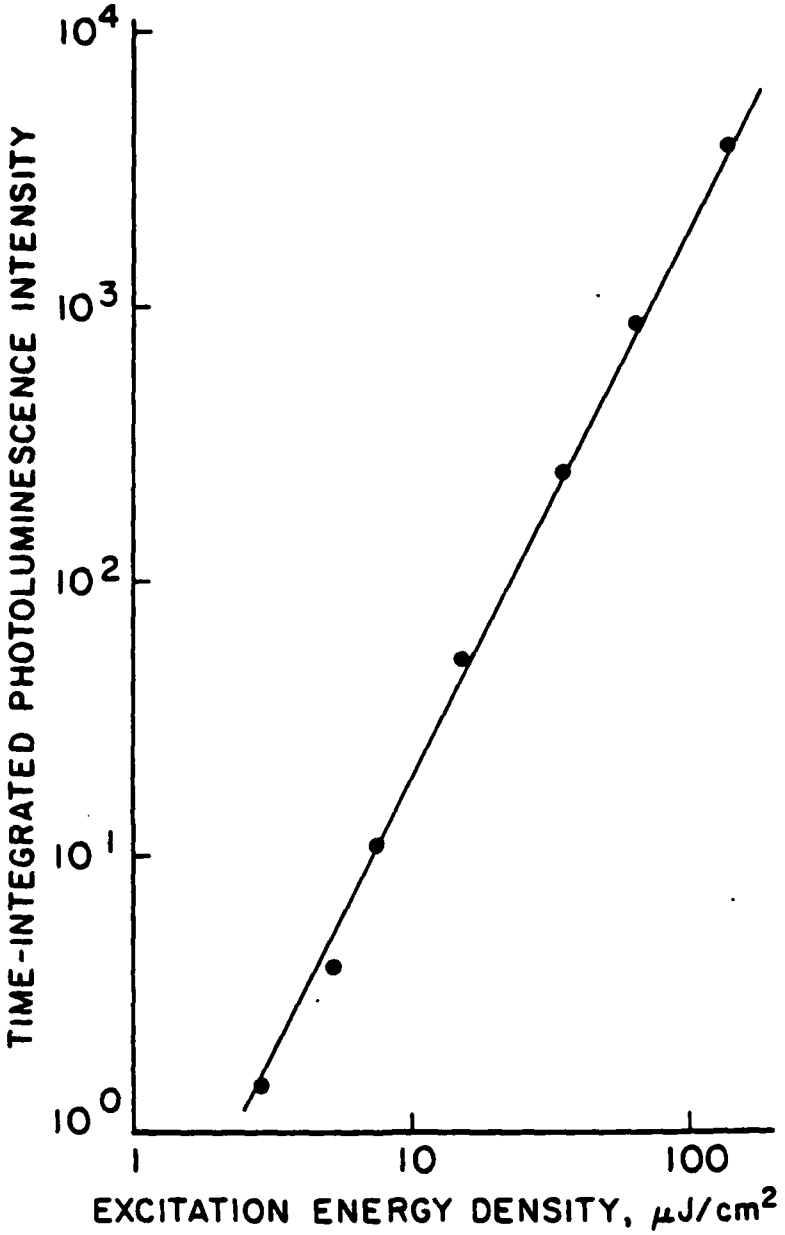

FIGURE 7

Room-temperature time-integrated photoluminescence intensity at the peak wavelength increases as the square of excitation energy density.

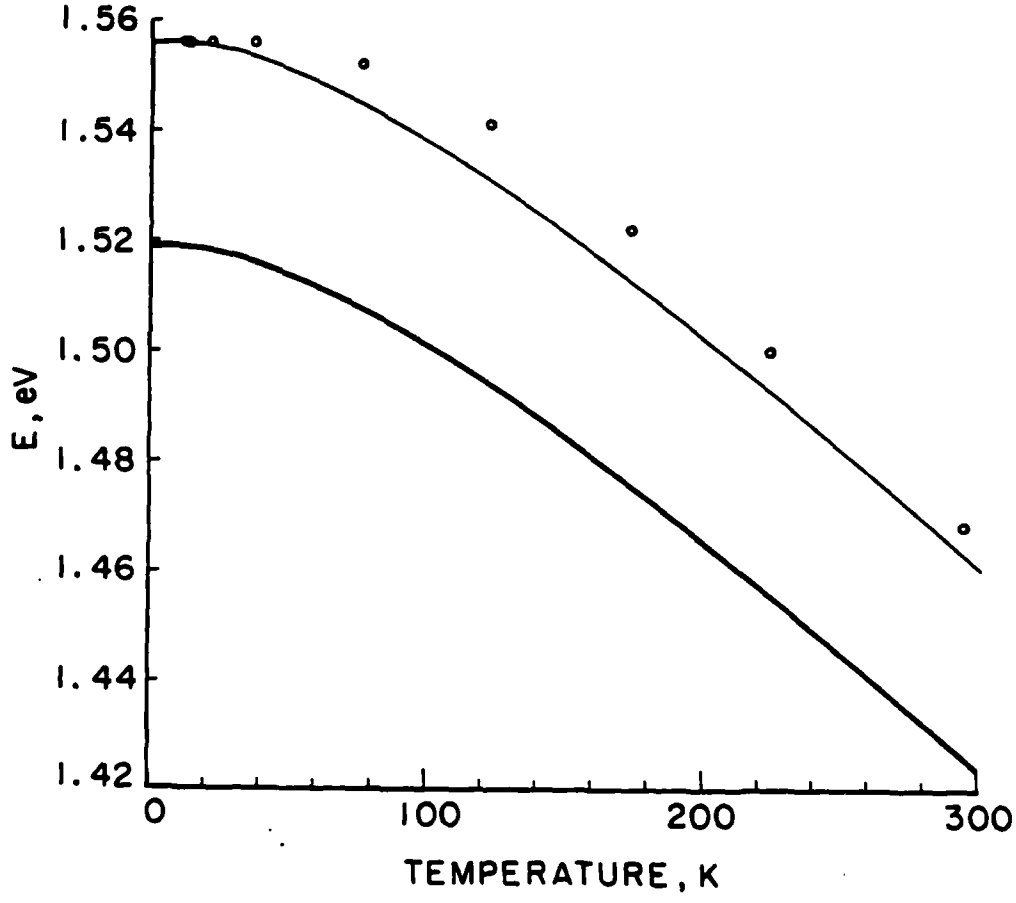

FIGURE 8

Photon energy of main peak vs. temperature for an excitation density of 20 $\mu J/cm^2$.

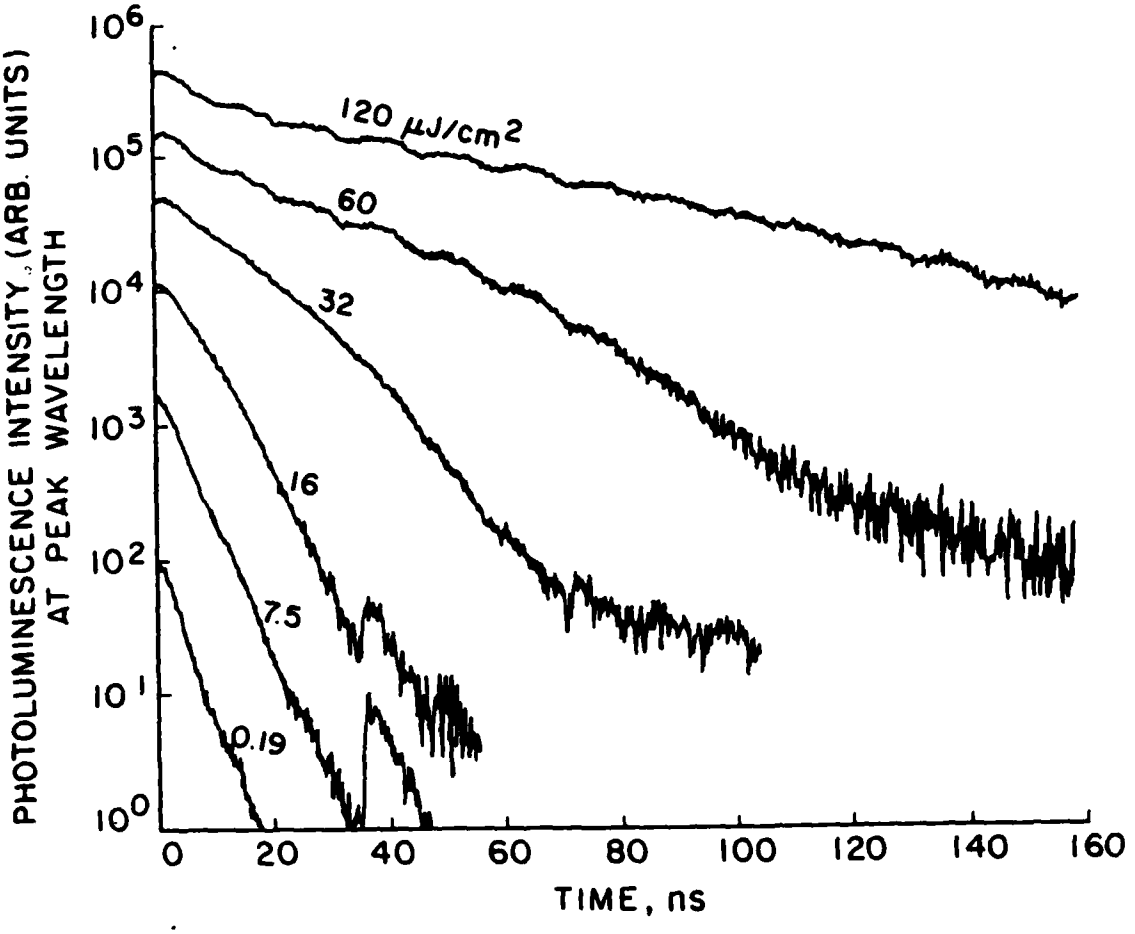

FIGURE 9

Time-resolved photoluminescence intensity at the peak wavelength is shown as a function of excitation energy density. The relative scaling of the different curves is only approximate, but each individual curve follows a consistent scale.

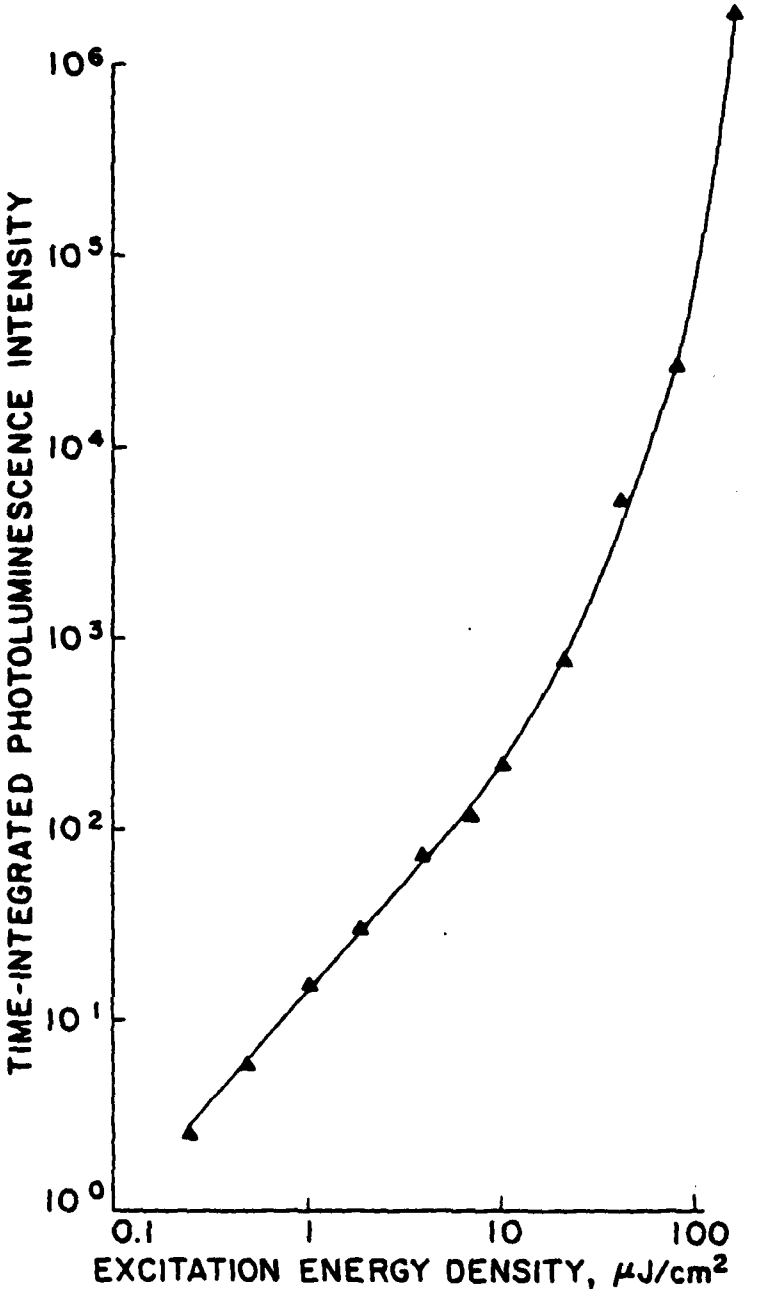

FIGURE 10

Time-integrated photoluminescence intensity at the peak wavelength is shown to increase superlinearly with excitation density past a threshold value.

Time-resolved photoluminescence of the main spectral peak is shown in Fig. 9. This is the first study of time-resolved photoluminescence in MOCVD-grown GaAs/$Al_xGa_{1-x}As$ quantum wells. The photoluminescence is quite slow overall (note time scale). The general character of short decays at low excitation and long decays at high excitation is typical of trap saturation. Carriers in the $n = 1$ quantum level in either the conduction or valence band quickly fall into a trap state. However, the number of trap states is limited, so that at high excitation the traps are filled and the carriers must stay in the $n = 1$ level and recombine at the slower radiative recombination rate. What is most unusual about these curves, however, is that the photoluminescence decay rate actually speeds up tens of nanoseconds after excitation. This behavior has not been observed previously in GaAs/$Al_xGa_{1-x}As$ quantum wells and is quite rare in the related bulk compounds. The most likely explanation for this behavior is that the carriers fall out of the trap states, making the trap states again available for carriers in the $n = 1$ level. Since the trap is then playing a larger role, the photoluminescence decay rate can speed up. A rate equation model has been developed to model this behavior. Preliminary results have qualitatively described the data well and have yielded a values of B in the range of a few times 10^{-11}.

The dependence of time-integrated photoluminescence on excitation density is shown in Fig. 10. Here the photoluminescence is relatively weak at low excitation densities, but at higher excitation the photoluminescence becomes much stronger as the traps are saturated and more of the recombination becomes radiative.

5. Magnitude of the Radiative Recombination Coefficient, B

Results from both samples show that B is no larger than a few $\times 10^{-10}$, and the more detailed MOCVD results suggest that B may be as much as an order of magnitude smaller. This makes B smaller than the corresponding value for bulk GaAs, a result which is initially surprising considering earlier predictions of a larger value of B due to the more favorable density of states situation in quantum wells.[7]. Recent work of Chang and Shulman[8] has shown that the matrix element for the $n = 1$ heavy hole transition in quantum wells is weaker than originally expected, and this factor may explain at least in part the small value measured here. The value of B is very important in the operation of semiconductor lasers, and if B is small, steps must be taken to insure high carrier densities within the quantum wells (such as wide collection areas which funnel down to a single quantum well) to insure good laser operation.

6. Future

Future work will investigate time-resolved and time-integrated photoluminescence in the samples at low (helium) and intermediate temperatures with a special focus on impurity luminescence. The nature of the trap state in the MOCVD material will be studied.

D. Optimal Achromatic Prism Beam Expanders—Theory and Design of Devices

When Klauminzer[9] introduced a prism beam expander into a pulsed dye laser in 1977, a century-old concept experienced a rebirth and has since found numerous applications in laser technology.[10] In particular, *achromatic* prism beam expanders have become important in broadband applications and arrangements requiring high wavelength stability.[11] The prism configuration, that is, which prism dispersions add (i.e., point "up") and which prism dispersions subtract (i.e., point "down"), while irrelevant in non-achromatic devices, is, of course, an important consideration in achromatic prism beam expanders.

For the purpose of improving the performance of the pulsed dye lasers in the tunable-laser-induced-grating experiment, we undertook a theoretical study of both achromatic and non-achromatic prism beam expanders.[12] One result of this study was that we were able to solve the previously-unsolved general problem of optimizing the efficiency (i.e., the transmission) of an N-prism not-necessarily-achromatic prism beam expander composed of arbitrary transparent materials for any given desired magnification. Using this result, we went on to show that, contrary to popular belief, any number of prisms (except for 1, of course) can produce an achromatic device, and interestingly, we found that the popular "compensating-pair-of-compensating pairs" (see Fig. 11) configuration is *not* in general the optimal achromatic four-prism beam expander. On the contrary, optimality is generally achieved by the somewhat unintuitive configurations in which the dispersions of the first $N-1$ prisms *add*, with the dispersion of the last prism subtracting (i.e, an *up-up-...-up-down* configuration; See Figs. 12, 13, and 14). In particular we discovered a unique *three-prism single-material achromatic beam expander*, using an up-up-down configuration, which should be especially useful for pulsed dye lasers in which the cavity length must be kept short. For other applications, up-up-...-up-down configurations of higher numbers of prisms were suggested. We showed that, for magnifications greater than about $[2-2/(2^{N-1}-1)]^N$ (i.e., about 2^N for large N), these arrangements always optimize the performance of achromatic N-prism devices of a single material. Finally,

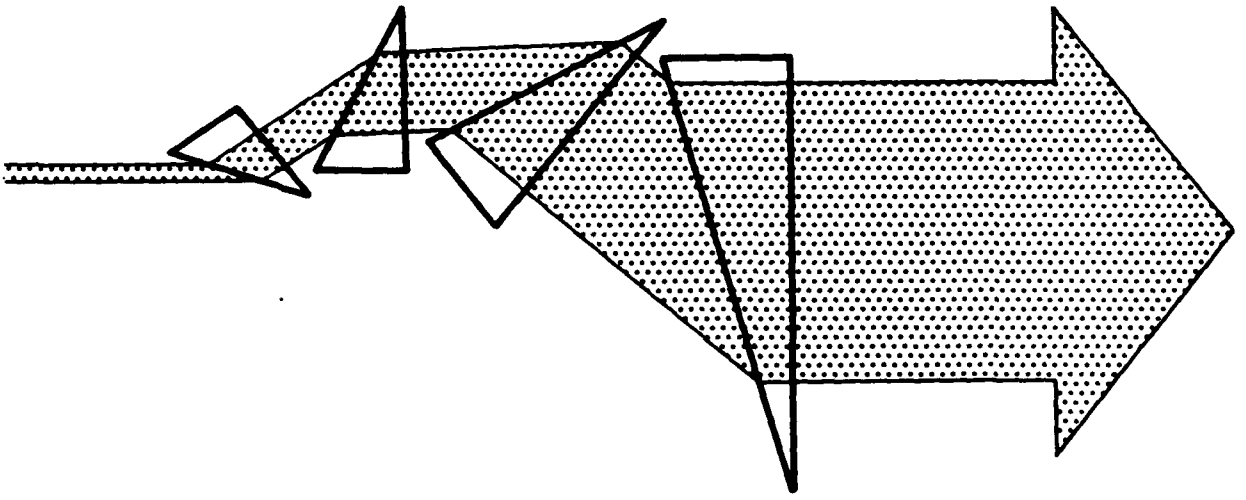

FIGURE 11

Standard down-up-up-down (compensating pair of compensating pairs) achromatic four-prism beam expander. This device consists of two pairs of nearly achromatic two-prism beam expanders, with the second pair inverted with respect to the first. It achieves nearly collinear input and output beams, but does not optimize transmission.

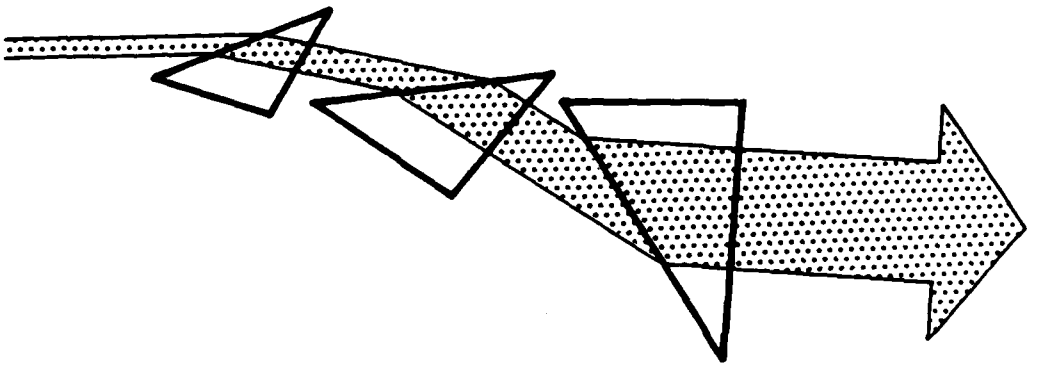

FIGURE 12

Three-prism up-up-down beam expander. This configuration is optimal for achromatic three-prism beam expanders.

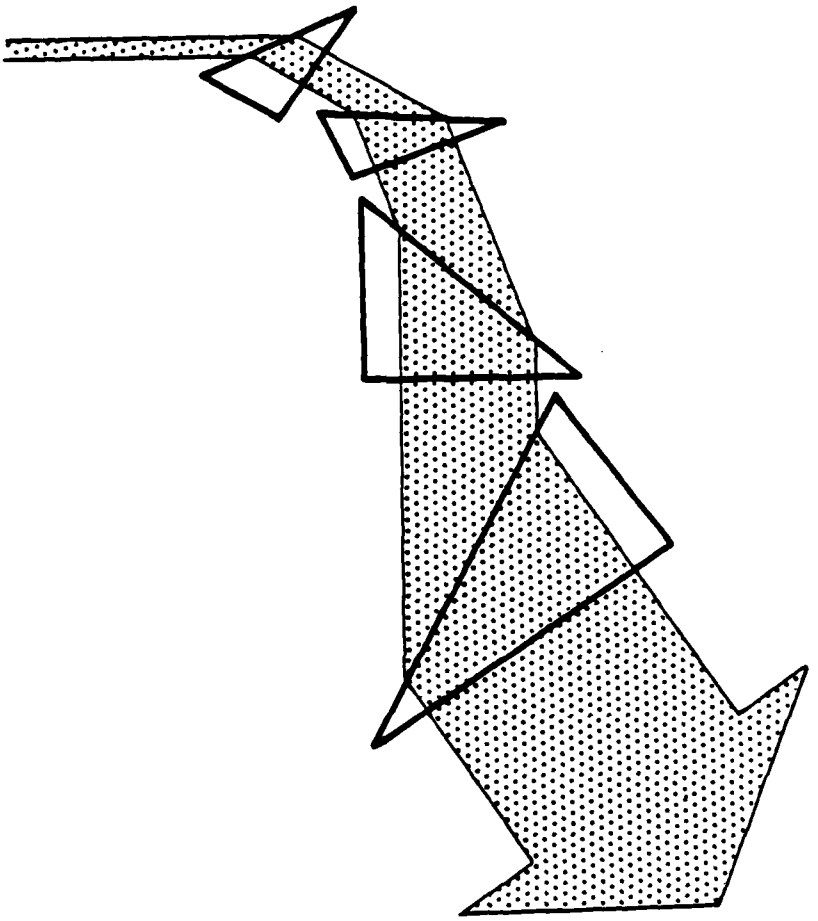

FIGURE 13

Four-prism up-up-up-down beam expander. This configuration is optimal for achromatic four-prism beam expanders of a single material with total magnification $\gtrsim 10$ and probably also for lower magnifications.

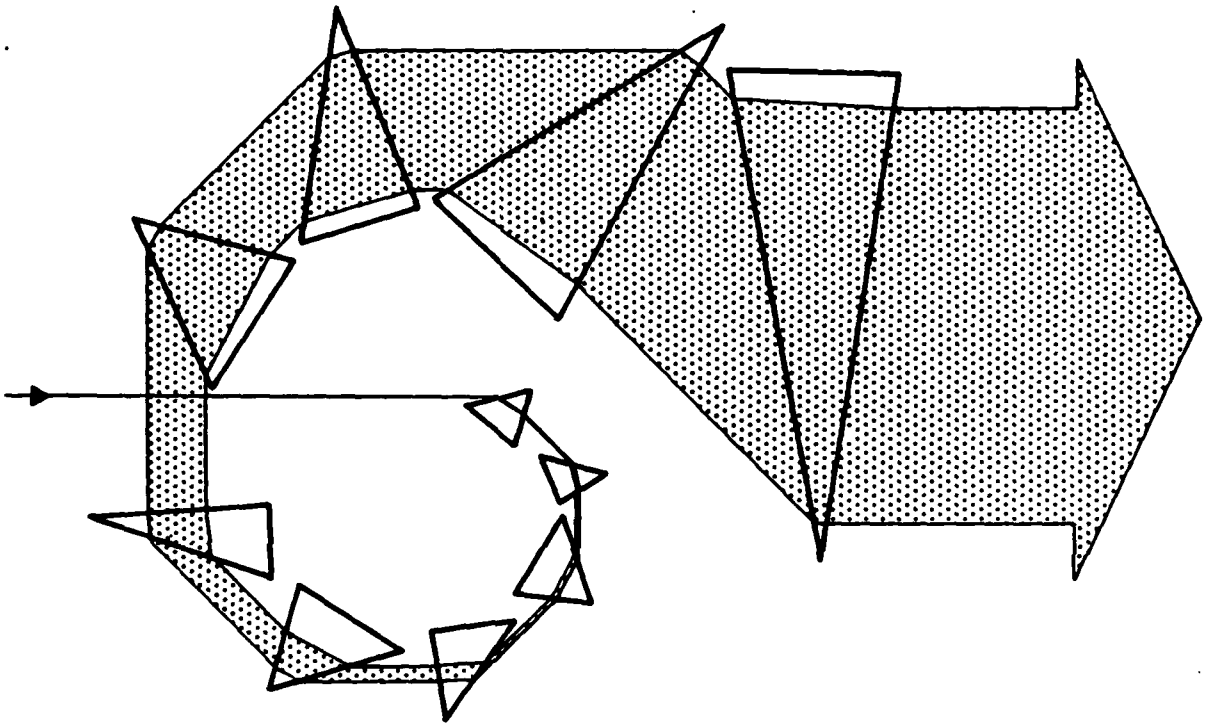

FIGURE 14

N-prism up-up-...-up-down beam expander. This configuration is optimal for achromatic single-material prism beam expanders of moderate to large magnification, specifically, for magnifications greater than about $[2 - 1/(2^{N-1} - 1)]^N$. In addition, if each prism magnification is 2, such a device achieves a total magnification of 2^N, a dispersion of $1/2^{N-1}$ that of a single prism, and a transmission of 98% per prism.

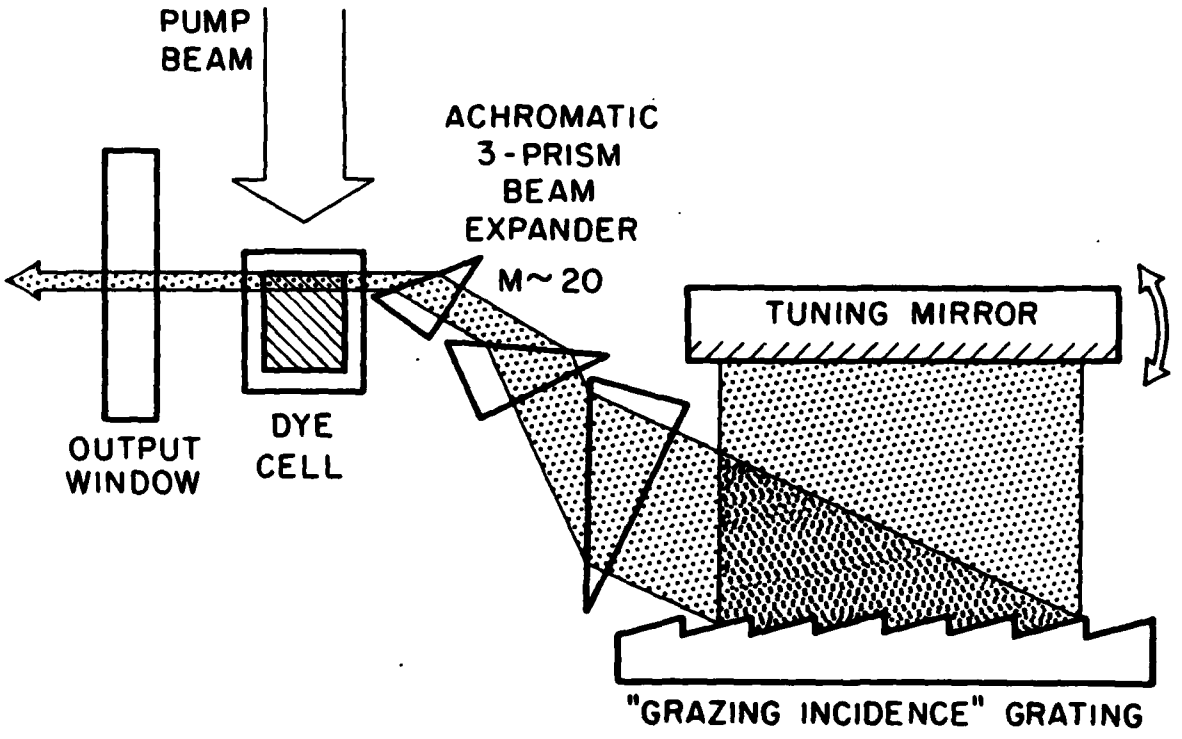

FIGURE 15

Three-prism (up-up-down) achromatic-prism-beam expander/grazing-incidence-grating dye laser. Such a hybrid design is more efficient than the prism-beam expander/Littrow-grating design or the grazing-incidence design. Use of a three-prism achromatic design should allow thermally stable single-mode operation and should further improve efficiency.

using these results, we were able to design an improved pulsed dye laser that combines the advantages of both the grazing-incidence and prism-beam-expander designs. Shown in Fig. 15, this design achieves greater efficiency for a given linewidth than any other design available.

III. REFERENCES

1. J. J. Song, J. H. Lee, and M. D. Levenson, "Picosecond Relaxation Measurements by Polarization Spectroscopy in Condensed Phases," *Phys. Rev. A* **17**, 1439 (1978).
2. G. L. Eesley, M. D. Levenson, and W. M. Tolles, "Optically Heterodyned Coherent Raman Spectroscopy," *IEEE J. Quantum Electron.* **QE–14**, 45 (1978).
3. R. C. Desai, M. D. Levenson, and J. A. Baker, *Phys. Rev. A* **25**, 1968 (1983).
4. R. Trebino, A. E. Siegman, and C. L. Ladera, "Suppression of Thermal Gratings in Polarization Spectroscopy," *J. Opt. Soc. Am.* **1**, 549 (1984).
5. H.C. Casey and M.B. Panish, *Heterostructure Lasers, Part A*, New York: Academic Press, 1978.
6. The excitonic luminescence argument was favored in P. Dawson, G. Duggan, H.I. Ralph, and K. Woodbridge, 17*th* International Conference on the Physics of Semiconductors, San Francisco, August 6–10, 1984; and P. Dawson, G. Duggan, H.I. Ralph, and K. Woodbridge, *Phys. Rev. B* **28**, 7381 (1983).
7. N. Holonyak, Jr., R.M. Kolbas, R.D. Dupuis, and P.D. Dapkus, "Quantum-Well Heterostructure Lasers," *IEEE J. Quant. Electron.* **QE–16** 170–186 (1980).
8. Y.C. Chang and J.N. Schulman *Phys. Rev. B* **31**, 2056, 2064, 2557 (1985).
9. G. K. Klauminzer, "New High-Performance Short-Cavity Dye-Laser Design," *IEEE J. Quant. Electron.* **QE–13**, 92D (1977).
10. F. J. Duarte, "Prism-Grating Systems for Laser Wavelength Measurements," *J. Phys. E: Sci. Instrum.* **16**, 599 (1983).
11. M. M. Fejer, G. A. Magel, and R. L. Byer, "High-Speed, High-Resolution Fiber-Diameter-Measurement System," *Appl. Opt.* to be published.
12. R. Trebino, "Achromatic N-Prism Beam Expanders: Optimal Configurations," *Appl. Opt.* **24**, 1130 (1985).

IV. AFOSR SPONSORED PUBLICATIONS AND CONFERENCE TALKS

1. P.M. Fauchet and A.E. Siegman, "Picosecond dynamics of dense hot electron-hole plasmas in crystalline and amorphised Si and GaAs," in *Ultrafast Phenomena IV*, Auston and Eisenthal, eds. Springer-Verlag, 1984, pp. 129–132.
2. P.M. Fauchet and A.E. Siegman, "Laser-induced surface ripples: recent developments," *J. Opt. Soc. Am.* **B1**, 455 (1984).
3. P.M. Fauchet and A.E. Siegman, "Ultrafast spectroscopy of very dense and hot electron hole plasmas in crystalline and amorphized semiconductors," to be published in the Proceedings of the 17th International Conference on the Physics of Semiconductors (1984).
4. P.M. Fauchet and A.E. Siegman, "Surface damage mechanisms in nontransparent media," to be published in the Proceedings of the 16th Annual Symposium on Optical Materials for High Power Lasers (1984).
5. P.M. Fauchet and A.E. Siegman, "Laser-induced surface ripples: what is understood and what is not," to be published in the Proceedings of the Materials Research Society Symposium A, Biegelsen, Rozgonyi and Shank, editors (1985).
6. P.M. Fauchet and A.E. Siegman, Topical Meeting on Ultrafast Phenomena, Monterey, June 1984, Paper WB7.
7. P.M. Fauchet and A.E. Siegman, International Quantum Electronics Conference (IQEC), Anaheim, June 1984, Paper MKK2.
8. P.M. Fauchet and A.E. Siegman, International Conference on the Physics of Semiconductors, San Francisco, August 1984, Paper FrP-C5.
9. P.M. Fauchet and A.E. Siegman, Symposium on Optical Materials for High Power Lasers, Boulder, October 1984, first paper, Tuesday session.
10. P.M. Fauchet and A.E. Siegman, Annual Meeting of the Materials Research Society, Boston, November 1984, Paper A3.7.
11. P.M. Fauchet, "Physics of semiconductors under very intense ultrashort laser pulse illumination," given at the University of Illinois at Chicago (3/23/84).
12. J.E. Fouquet and A.E. Siegman, "Recombination Times in GaAs/$Al_xGa_{1-x}As$ Multiple Quantum Well Structures," *Proceedings of the 17th International Conference on the Physics of Semiconductors*, San Francisco, California, August 6-10, 1984.

13. J.E. Fouquet and A.E. Siegman, "Room Temperature Photoluminescence Times in a GaAs/$Al_xGa_{1-x}As$ Molecular Beam Epitaxy Multiple Quantum Well Structure," *Appl. Phys. Lett.* **46**, 280, (1984).
14. J.E. Fouquet, A.E. Siegman, R.D. Burnham and T.L. Paoli, "Carrier Trapping in Room Temperature Time-Resolved Photoluminescence of a GaAs/$Al_xGa_{1-x}As$ Multiple Quantum Well Structure Grown by Metalorganic Chemical Vapor Deposition," *Appl. Phys. Lett.* **46**, 374, (1984).
15. R. Trebino, A. E. Siegman, and C. L. Ladera, "Suppression of Thermal Gratings in Polarization Spectroscopy," International Conference on Quantum Electronics (IQEC), Anaheim, California, June 1984.

V. PROFESSIONAL PERSONNEL

Professor A. E. Siegman is on sabbatical leave in West Germany for the academic year, and Professor S. E. Harris has been appointed co-principal investigator in his absence.

Professor P. M. Fauchet, Dr. Rick Trebino, and graduate students Julie E. Fouquet, Charles E. Barker, and David C. Nabors were associated with the research on this contract during this period. Professor Fauchet has since taken up a faculty position at Princeton University.

VI. HONORS, AWARDS, AND OUTSIDE INTERACTIONS

The principal investigator on this contract, Professor A. E. Siegman, was awarded a Senior U.S. Scientist Award by the Humboldt Foundation, and has been at the Max Planck Institute in Munich, Germany on sabbatical leave over the past year. During this period he was also elected a Fellow of the American Academy of Arts and Sciences.

END

FILMED

11-85

DTIC